Mixing, rheology, and stability of highly filled thermal pastes

C. Feger
J. D. Gelorme
M. McGlashan-Powell
D. M. Kalyon

Thermal pastes play an important role in transmitting heat generated by an integrated circuit chip from its back side to a cooling cap or heat sink which transfers the heat to the environment. Most thermal pastes are formulations of solid, thermally conducting particles in a liquid matrix loaded to very high solids content. The mixing process for such pastes is complex but important, since it determines several of the paste properties. In particular, paste rheology is related to the work imparted to the paste during the mixing process. It determines the minimum bondline between solid surfaces that can be attained with a particular paste during the assembly process, which is essentially a squeeze flow process. Paste stability depends on the amount of entrapped air incorporated during the mixing process; this is demonstrated by infrared (IR) visualization of the degradation of air-containing paste in a computer-chip–heat-sink gap and the absence of this degradation mechanism in vacuum-mixed paste. This paper describes two different mixing processes for highly filled thermal pastes, the associated changes in their rheological behavior, and paste degradation in chip–heat-sink gaps during thermal stressing.

Introduction

Thermal pastes consist of thermally conducting solids, such as metals, ceramics, and/or carbon, which are incorporated into liquids that include various hydrocarbons or silicone oils [1–3]. Additionally, other ingredients such as antioxidants and/or phase stabilizers are often present in small amounts [4]. For the highest thermal conductivities, the degree of loading of the solid ingredients is maximized to be as close as possible to the maximum packing fraction. This is achieved by tailoring the particle shape and size distributions of the solid ingredients, principally by employing bimodal or multimodal particle size distributions [5]. The concentration of solids in thermal paste generally exceeds 70 vol.%.

It is generally understood [6] that the degree of solids loading is related to the maximum bulk thermal conductivity, k, of the paste. Less appreciated is the fact that the degree of mixing achieved by the mixing process influences k to a significant degree. While there is a large body of knowledge about mixing of high solids composites in such separate areas as solid rocket fuels and propellants [7–10], electrically conductive compounds [11], composites [12, 13] and soaps [14], little if anything has been reported about mixing of thermal pastes. In this paper, we review the relevant facts which apply to the mixing of thermal pastes.

Similarly, only a few studies [15–21] exist on the rheology of thermal pastes, although their flow behavior is critical in attaining the narrow gap thickness required to reduce the thermal resistance between a computer chip and a cooled surface, or "hat." Most reported studies [15–21] have been carried out on highly filled systems of a very different nature, such as phase-change materials [15], thermal gels [16], and other polymer-based systems [17–21]. In this paper, we discuss what is relevant to understanding the rheology of thermal pastes.

Possibly the most important property of thermal paste is the long-term stability of its thermal resistivity imparted to the gap between a chip and the cooling hat.

©**Copyright** 2005 by International Business Machines Corporation. Copying in printed form for private use is permitted without payment of royalty provided that (1) each reproduction is done without alteration and (2) the *Journal* reference and IBM copyright notice are included on the first page. The title and abstract, but no other portions, of this paper may be copied or distributed royalty free without further permission by computer-based and other information-service systems. Permission to *republish* any other portion of this paper must be obtained from the Editor.

0018-8646/05/$5.00 © 2005 IBM

This property is rather unique to thermal pastes, since most highly filled composites used in the areas mentioned above [7–14] exist in the liquid phase only during a short transition period (primarily during processing). Therefore, we describe in more detail how the stability of thermal pastes is measured and how to improve this property that is critical to the electronics industry.

Experimental information

Two different types of mixers and associated mixing procedures were applied to the processing of the thermal paste. First, the mixing was carried out using a modified intensive mixer with counter-rotating roller-type agitator blades, i.e., the Model EU-5V torque rheometer from Haake Buchler Instruments, Inc., Saddle Brook, NJ. This tool has a 60-cc mixing chamber; it was operated at a roll speed of 32 rpm and at 50°C. Two separate procedures involving mixing with and without the application of vacuum were applied. The second mixing process involved the use of a planetary mixer (Model LDM-2 from Charles Ross & Son, Hauppauge, NY) followed by the application of three-roll milling with a gap size down to 150 μm using a Model SDA three-roll mill (Buhler, Minneapolis, MN; see *www.buhlergroup.com*).

The mixing index values of the resulting mixtures were characterized at a scale of examination range of 7 mm^2 to 80 mm^2 using wide-angle X-ray scattering employing a Rigaku MiniFlex diffractometer (*www.msc.com*) in conjunction with a CuK_α radiation source operated at 30 kV. For a finer scale of examination of 0.001 mm^2, a LEO 982 digital scanning electron microscope (SEM) operated at 1 kV was used.

The rheological properties of the various pastes were measured using an ARES rotational rheometer from Rheometrics (now TA Instruments, New Castle, DE). Samples were characterized at 50°C if not otherwise indicated. Dynamic properties were measured under small-amplitude oscillatory shear flow, and steady-flow behavior was characterized using steady torsional flow. Strain sweep tests were conducted at a frequency of 1 rps. All experiments used 25-mm-diameter disks in parallel-plate configuration. For most experiments we used stainless steel disks with smooth surfaces. In a few steady-flow experiments we used a parallel-plate combination of a smooth or rough Cu surface on one side and a back-side silicon surface on the other disk in order to simulate the surfaces in a chip–cooling-cap gap. These surfaces were obtained by gluing respective specimens to the stainless steel disks.

The IR camera used for imaging was a Merlin Mid from FLIR Systems, Indigo Operations (Goleta, CA) with a 320 by 256 InSn focal plane array detector with a spectral range of 3–5 μm. While the accuracy of the temperature reading is $\pm$1°C or 2%, whichever is lower, temperature fluctuations of $<$0.1°C can be resolved. The spatial resolution can be as small as 8 μm when a 1$\times$ microscope lens is used. The detector area is 30 μm $\times$ 30 μm.

Mixing of thermal pastes

The thermal pastes used for this study consist of a highly filled suspension consisting of aluminum and alumina particles incorporated in hydrocarbon oil. Two formulations with differing solid contents were mixed and investigated. The solid contents are greater than 72 vol.%.

Mixing is a complex procedure that can be carried out either in a batch or in a continuous process [22, 23]. In this project we used two different batch-mixing processes and compared the results. One process was carried out first using a planetary Ross mixer and then completing the mixing process using a three-roll mill [24]. The finished product was degassed for two hours in a vacuum oven at 30 torr using a programmed temperature ramp from room temperature to 200°C. Degassing in this fashion minimizes the amount of co-mixed air but does not eliminate it (see below). To do that, high-shear mixing under vacuum is required. The overall mixing process takes considerable time and is operator-dependent.

The second batch process used high-shear mixing in the torque rheometer, with mixing times varied from 5 to 20 minutes. A significant advantage of this process is that the mixing of the ingredients can be carried out under vacuum. Air removal from the paste during the mixing process is important, as is shown below.

The goal of mixing is to achieve a uniformly mixed sample. However, uniformity is arbitrarily defined and depends on the scale of the investigation [8]. Since the amount of material used per chip in the narrow gap between the chip and the cooling cap (bondline) is rather small (of the order of 0.1 μl), the mixing quality has to be very high. Mixing quality is characterized by a random distribution of particles within the mixture and small average distances between the various components.

Degree of mixedness analysis

The following provides background for the analysis of the degree of mixedness of the solid ingredients of the thermal paste samples. During determination of the degree of mixing experiments, N measurements of the concentration of one of the ingredients, c_i, of the formulation are made to determine the mean, $\bar{c}$, and the variance, s^2, of the concentration distribution of this ingredient. The difference between the mean concentration, $\bar{c}$, and the known overall concentration, ϕ, of an ingredient (minor or major component) indicates the quality of the sampling technique.

The variance, s^2, arising from the distributions of the individual concentration values (i.e., c_i measurements)

provides the most basic measure of the homogeneity of a mixture. A small variance value suggests that the mixture approaches the behavior of a homogeneous system, in which most of the samples yield concentration c_i values that are approaching the mean concentration, $\bar{c}$, of all samples. If the components of a mixture are completely segregated, maximum variance occurs. The value of the maximum variance (or the square of the between-sample standard deviation) for a completely segregated system can be defined by assuming that the samples are taken either from one component or from the other without crossing a boundary [25]:

$$s_0^2 = \bar{c}(1 - \bar{c}). \quad (1)$$

The most ideal state of random mixing possible is achieved when the variance of the concentrations of the targeted ingredient sampled from different locations in the mixture reaches the variance of the binomial distribution. The present study used the mixing index, MI, which is based on the standard deviation of the distribution of the concentration of one of the ingredients of the formulation over the standard deviation of the completely segregated sample for the same ingredient [11]. This mixing index exhibits a value of 0 for a completely segregated sample, and its value approaches 1 for a completely random distribution of the concentrations of its ingredients:

$$MI = 1 - \frac{s}{s_0}. \quad (2)$$

Two basic mixing mechanisms exist: extensive or distributive mixing and intensive or dispersive mixing. The quality of distributive mixing is determined by the spatial distributions of the phases, affected by the amount of strain a sample experiences during mixing and the reorientation of the interfaces between the phases. The extent of dispersive mixing is determined by the stress distribution and the stresses that are applied on the phases to change their physical properties, including the particle size distribution of the solid phase [26]. The efficiency of the dispersive mixing process in reducing agglomerate sizes increases with the use of smaller gaps between mixing blades or rolls and binders with higher viscosity values. The mixing of highly filled systems containing small particles involves both distributive and dispersive types of mixing. In the case at hand, distributive mixing is considered to be the predominant mode.

Mixing results

Table 1 shows a comparison of the mixing indices of the two main components of the pastes mixed by the torque rheometer under various conditions and by the planetary Ross mixer followed by the three-roll-mill mixing. The MI values of the main ingredients are identical for the two mixing methods. However, with the torque rheometer, this mixing index is obtained after only 5–15 minutes of mixing compared with approximately two hours required for batch component mixing with the planetary/three-roll-mill process combination. Furthermore, although wide-angle X-ray scattering experiments [8] indicated that the distributive mixing characteristics of the pastes prepared by the different mixing methods were very similar, at the finer scale of examination of SEM image analysis, the samples mixed with the torque rheometer were found to be better mixed distributively than those processed by the three-roll mixer.

As is shown next, the rheological characterization of the mixtures revealed that the shear viscosity of the samples mixed with the planetary/three-roll mixers was greater than that of the samples processed with the torque rheometer. The thermo-gravimetric analysis of the two pastes showed comparable oil contents, thus eliminating differences in binder content as a possible explanation for the higher shear viscosity found in the three-roll-mixed samples. It remains unclear, however, whether the dispersive mixing characteristics of the two pastes are different, since the higher shear stresses of the torque mixer are expected to impart smaller agglomerate sizes and therefore smaller values of yield stress and shear viscosity.

Table 1 Mixing index (MI) and coefficient of variation (CV) values for components 1 and 2 for differently mixed pastes. Torque-rheometer-mixed samples, their mixing times, and mixing conditions with (w) or without (w/o) vacuum are identified by TQR (mixing time in minutes/w or w/o); the sample mixed using the Ross mixer followed by three-roll milling is identified as 3RM.

Sample name	*Component 1*		*Component 2*	
	MI	*CV*	*MI*	*CV*
TQR (5/w)	0.92	0.07	0.94	0.07
TQR (15/w)	0.96	0.03	0.97	0.04
TQR (5/w/o)	0.96	0.04	0.97	0.04
TQR (15/w/o)	0.92	0.07	0.96	0.04
3RM	0.96	0.04	0.97	0.03

The coefficient of variation, CV, is the standard deviation of the distribution, s, over the mean concentration, $\bar{c}$; i.e., $CV = s/\bar{c}$.

Rheological characterization

Strain sweep tests showed that the paste exhibits linear viscoelastic behavior only up to a strain value of 0.1%. At larger values of strain, the storage modulus, G', which characterizes the energy stored as elastic energy during one cycle of deformation (solid-like behavior), the loss modulus, G'', which characterizes the energy dissipated as heat during one cycle of deformation (liquid-like

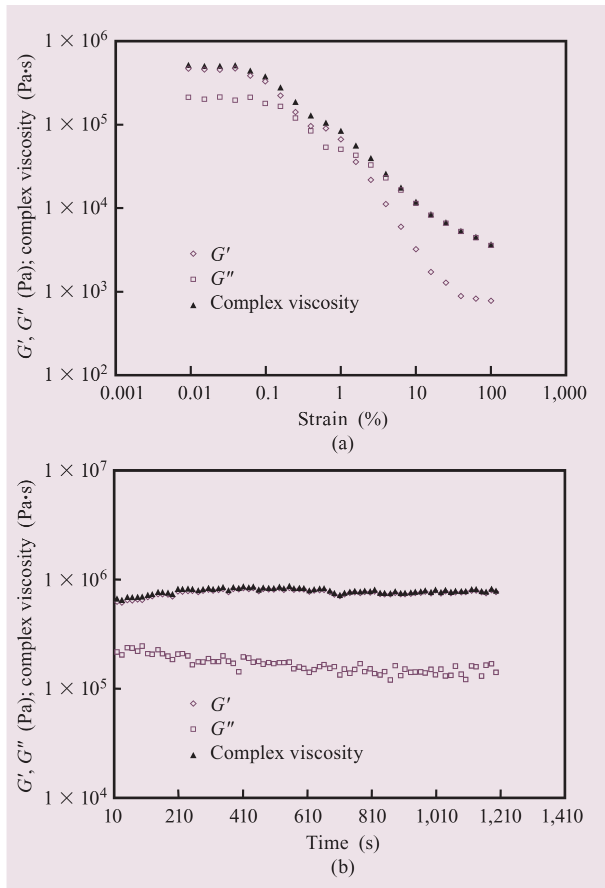

Figure 1

(a) Strain sweep curves of the torque-rheometer-mixed paste at 1 rps. Storage modulus (G') and loss modulus (G'') in Pa and magnitude of complex viscosity in Pa•s are displayed. (b) Time sweep curves of the torque-rheometer-mixed paste at 0.02% strain and 1 rps.

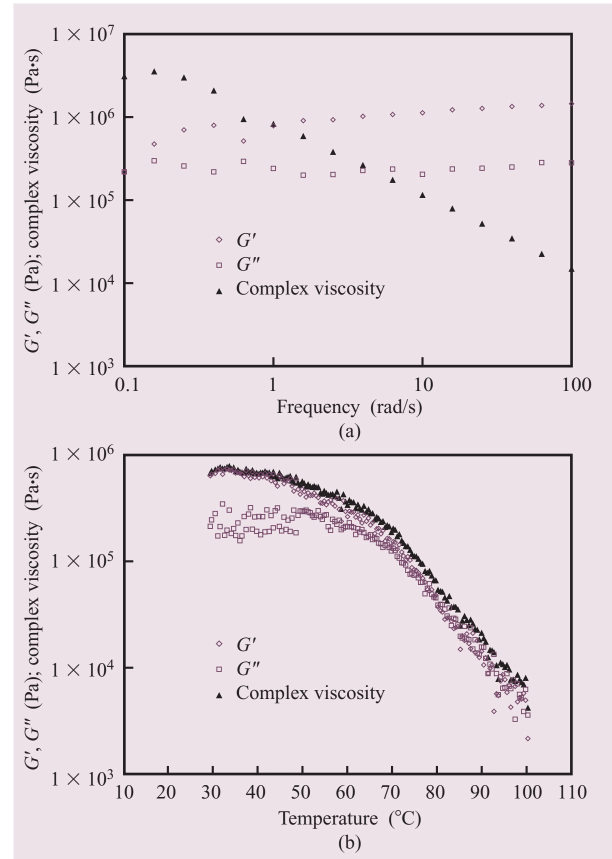

Figure 2

(a) Frequency sweep test of the torque-rheometer-mixed paste. (b) Dynamic temperature sweep test at 1 rps and 0.02% strain.

behavior), and the magnitude of the complex viscosity of the thermal paste (which approaches the zero shear viscosity of the thermal paste as the deformation rate is reduced) exhibit sharp drops, as shown in **Figure 1(a)**. Hence, oscillatory shear tests were conducted at strain amplitudes lower than 0.1%.

At relatively large strains, the appearance of a discontinuity in the straight marker line at the material–wall interface was observed, providing visual evidence of wall slip, a characteristic of highly filled systems [27, 28]. Wall slip in concentrated suspensions occurs on the basis of the formation of an apparent slip layer, which consists solely of the binder of the suspension. The thickness of the apparent slip layer is generally a fraction of the particle size of the solid phase [29]. Wall slip increases with increasing thickness of the apparent slip layer, decreasing shear viscosity of the binder, and increasing amount of air incorporated into the suspension [30, 31]. Wall slip was negligible in the linear viscoelastic range of the small-amplitude shear experiments.

Wall slip is a significant failure mode of thermal pastes; in vertical geometries it can lead to the loss of all or part of the thermal paste from a chip–cooling-hat gap [27–32]. Roughened surfaces can be used to counteract wall slip. However, it has been shown by Aral and Kalyon [28] that attempts to deform viscoplastic suspensions using roughened surfaces can lead to the development of internal slip planes and the fracturing of the paste during shearing. As part of the present study, we tested whether the investigated paste will fracture in steady shear using roughened Cu surfaces, and we have confirmed that this system does indeed develop near-surface and bulk cracks under certain conditions.

The paste mixed with the torque rheometer was subjected to time sweeps at 0.02% strain and 1 rps frequency to determine its stability. The dynamic properties remained largely unchanged during this

test, indicating that the material is stable over extended durations of time under oscillatory shear flow [**Figure 1(b)**].

The frequency sweep test revealed that the loss and storage modulus values are generally parallel, with the storage modulus values significantly greater than the loss modulus values over the entire frequency range of 0.1 to 100 rps [**Figure 2(a)**]. This behavior is characteristic of the gel-like structures formed by the high degree of solid fill. The magnitude of the complex viscosity exhibits a decrease with increasing frequency. Frequency sweep tests were conducted with at least three different samples to validate the repeatability of the results and to identify the sample-to-sample variation, which was found to be small.

The dynamic properties during temperature sweep experiments are shown in **Figure 2(b)**. The sample is sheared at 1 rps and 0.02% strain as the temperature is gradually increased. The dynamic properties exhibit a rather sharp decrease with increasing temperature.

The samples were also subjected to steady torsional flow experiments at three different shear rates at 50°C. Again, the material showed very significant wall slip at the three apparent shear rates, as revealed by the straight-line marker technique (**Figure 3**). There is no deformation of the specimen at shear stress values that are less than about 40 kPa, suggesting that the yield stress of the thermal paste is in the 20–40-kPa range. The yield stress value of the thermal paste was found to change as a function of the mixing conditions.

Samples mixed under vacuum for 5, 10, and 15 minutes in the torque rheometer were subjected to a frequency sweep test, and the results of the rheological characterization are compared in **Figure 4**. All samples exhibit very similar magnitudes of complex viscosity, indicating that the structure and hence the rheological behavior of the paste remained more or less invariant after the first five minutes of mixing. This suggests that acceptable degrees of mix can be achieved during a relatively short residence time in the torque rheometer. It suggests further that particle coating and agglomeration breakdown are essentially complete after five minutes.

The sample mixed using the planetary Ross mixer followed by the three-mill-roll process was also characterized using frequency sweep measurements, and exhibited a significantly greater magnitude of complex viscosity values. This indicates either that the particles were not as homogeneously coated with the binder as those mixed with the torque rheometer, or that the binder content of the mixtures arising from the planetary Ross mixer was lower than that mixed using the torque rheometer. Thermo-gravimetric analysis showed that the binder content of the suspensions remained constant during mixing, indicating that it was the difference in the degree of mixedness of the ingredients that gave rise to the observed difference in the rheological behavior of the thermal pastes mixed by the two different methods. If during mixing the binder does not coat the individual particles but rather the agglomerates of the particles, the voids found between the particles in the agglomerates act to increase the overall effective volume percentage of solids (the volume occupied by the particles and the void space between the particles) to give rise to an increase

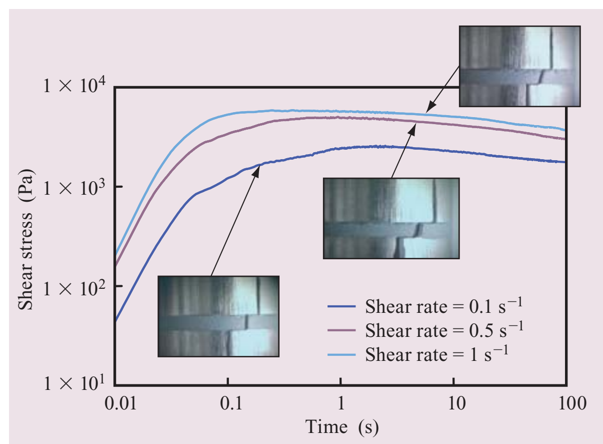

Figure 3

Steady torsional flow experiments at various shear rates and 50°C. The photo insets show that at a targeted apparent shear rate of 0.1 s^{-1}, wall slip is near 100% with no sample shearing, but that sample deformation increases at higher apparent shear rates while wall slip continues to be significant.

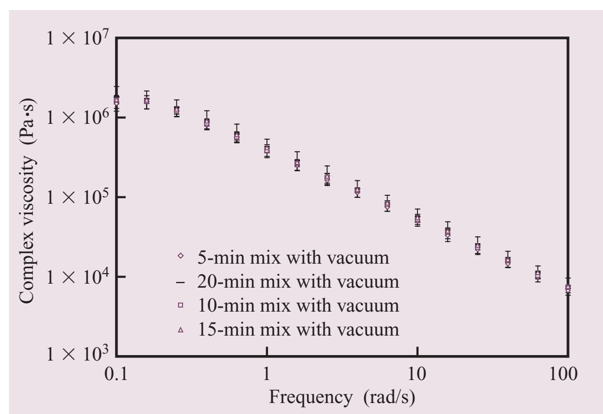

Figure 4

Frequency sweep test of samples mixed under vacuum for 5, 10, and 15 minutes. Only the magnitude of complex viscosity is displayed.

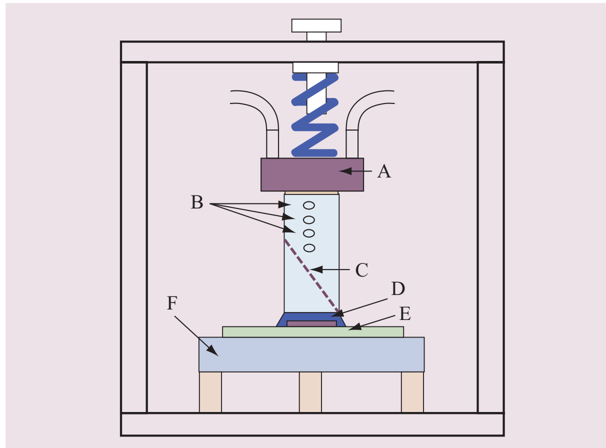

Figure 5

Schematic of the silicon heat-sink assembly. The IR camera is placed at 90° to the thermocouples. A: water-cooled cold plate; B: thermocouple holes; C: silicon rod split in half and gold-plated; D: thermal interface material (TIM); E: chip and chip substrate (light green); F: socket. The assembly is in a frame to apply pressure to achieve the desired TIM bondline thickness.

in the yield stress and hence the shear viscosity of the suspension. On the other hand, when the binder drives out the air during the mixing process and the individual particles are coated (i.e., encapsulated) with the binder, the yield stress and the shear viscosity of the suspension decrease.

Infrared (IR) imaging

Infrared imaging or IR thermography [33, 34] is a technique in which the thermal map of an object is generated from the infrared radiation it emits. The emitted radiation is collected with special IR optics consisting of germanium, silicon, or sapphire elements and is detected by an IR detector or a focal plane array of detectors (InSn, etc.). The temperature of the object is determined by using Planck's law [35, 36]. The spectral range of the used IR wavelengths depends on the emissivity of the object surface [37], detector sensitivity, and atmospheric absorption. IR images obtained in this way reflect the spatial distribution of temperature on the object surface. This method is well suited to studying the temperature distribution of processor chips in operation.

Failure of the thermal paste under operating conditions is known to cause processor failure. The mechanism of paste failure is not well understood; consequently, a silicon prism heat-sink assembly was developed that enables IR imaging of the thermal interface in the actual packaging environment. This silicon heat-sink assembly (**Figure 5**) comprises two matching right-angle prisms with one prism coated with gold along the surface of the hypotenuse such that the IR from the heat source (i.e., the chip) is reflected into an IR camera. The second prism is bonded to the first to form a cube. The top surface is bonded to a cold plate through which a coolant is circulated. The heat flow in this assembly is from the chip through the thermal paste through the bottom of the cube to the sink at the top of the cube.

IR imaging was performed on a POWER4* microprocessor running at up to 140 W; 100 μm (4 mils) of the roll-milled thermal paste was applied to the back side of the chip. The prism was pressed on top of the paste until the desired gap was obtained. IR images of the heat-sink–paste interface were taken at various powers from room temperature (0 W up to 125 W). Initially the paste appearance was fairly uniform [**Figure 6(a)**]. As the power reached 124 W, defects appeared [**Figure 6(b)**]. The temperature of these defect regions was about 10°C to 20°C above the background and was close to the

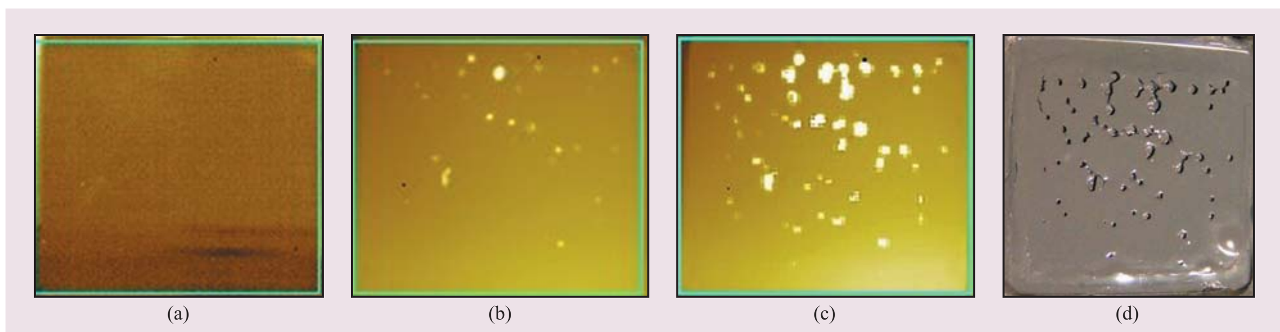

Figure 6

IR images of thermal paste (a) after application between chip and Si heat sink; (b) after the chip power reached 124 W; (c) after keeping at temperature for seven days. (d) Optical image of sample (c) after heat-sink removal. In the IR images, lighter shades of yellow indicate higher temperatures, darker shades lower temperatures.

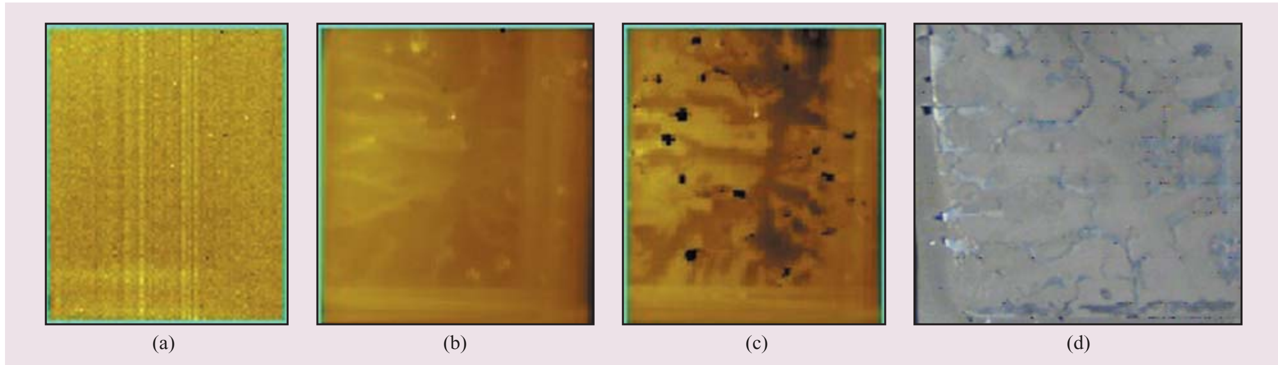
(a) (b) (c) (d)

Figure 7

IR images of vacuum-mixed thermal paste (a) after application between chip and Si heat sink; (b) after 18 hours at 78 W (84°C) (light horizontal lines in the middle and at the upper left are oil-rich erosion channels); (c) after six days of power cycling between 45 W and 98 W. (d) Optical image of sample (c) after heat-sink removal.

temperature of the built-in chip temperature sensor near the area of the chip with the highest power density (hot spot). The defect regions were investigated by optical microscopy of the dissembled sample [**Figure 6(d)**] and were found to be voids that extend through the entire thickness of the paste.

The voids formed initially were small. Over time at temperature they grew larger and eventually began to coalesce [**Figure 6(c)**]. Defect density and growth were most severe over the chip hot spots. It is believed that these voids originate from air inclusions in the thermal paste. To verify the effect of included air on the degradation behavior, a sample mixed in the torque rheometer under vacuum was investigated. This sample showed a void present from the beginning and associated with placing the sample on the chip; this void did not grow during subsequent heating [**Figure 7(a)**]. However, another paste-degradation process, best described as *paste erosion*, was observed [**Figure 7(b)**]. This mechanism has been widely observed in pastes that were not vacuum-mixed; it is an intrinsic failure mechanism of thermal pastes. The factors leading to paste erosion are not yet completely understood.

The thermal paste contains oil as the liquid phase, and this oil forms a thin film on the chip–paste interface and the paste–heat-sink interface (the slip layer, as discussed above). In order to understand the effect of this layer in paste voiding, a thin layer (~1 μm) of a transparent infrared fluid was placed between chip and prism heat sink. IR images of the fluid interface were acquired while the chip was power-cycled. Sudden and rapid void formation was observed in the oil as the microprocessor power dropped from 136 W to 83 W. These voids originated at the edge of the microprocessor and traveled inward toward the center of the microprocessor on a scale of milliseconds. Such voids were often closed off from the outside, creating pockets of air between chip and silicon heat sink (**Figure 8**). Thus, it is clear that the void formation is to some extent related to the rheological behavior of the binder, and in future experiments the effect of higher oil viscosity on void formation will be investigated.

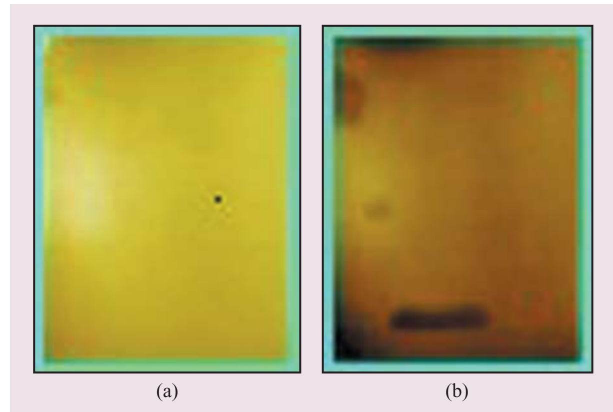
(a) (b)

Figure 8

IR images of thermal oil in a chip–heat-sink gap (a) before (power = 136 W, T_{avg} = 89°C) and (b) after (power = 83.6 W, T_{avg} = 55°C) sudden temperature drop. The dark shadows at the upper left and at the bottom of part (b) indicate where air pockets have formed in the oil of the chip–heat-sink gap during rapid cooling. [The dark spot in the middle of part (a) is an artifact caused by a defective pixel.]

Concluding remarks

In this paper we have described the mixing process, intrinsic properties, and degradation behavior of a highly

filled thermal interface material. The results strongly suggest that high shear mixing is essential in producing highly dispersed pastes with rheological properties that permit the smallest possible bondline between a chip and metal plate (e.g., a cooling hat) to be achieved. Investigation of thermal paste degradation by IR imaging further suggests that mixing should be conducted under vacuum to remove air from the paste, since included air can result in void formation that degrades the thermal performance of the paste. Void formation can also be affected by the behavior of the interfacial oil layer.

Acknowledgments

This project was facilitated through the participation, in one capacity or another, of many individuals to whom we are grateful. Sushumna Iruvanti and Tuknekah Noble of IBM and H. Gevgilili, E. Birinci, M. Erol, M. Cimen, and B. Greenberg of the Stevens Institute of Technology contributed to the testing of the materials and information. Matthew Farinelli and Joseph Zinter helped in the development of the IR setup. The help and support of S. Buchwalter is greatly appreciated.

*Trademark or registered trademark of International Business Machines Corporation.

References and note

1. N. G. Aakalu and L. A. Rittmiller, "Non-Bleeding Thixotropic Thermally Conductive Materials," U.S. Patent 4,265,775, May 5, 1981.
2. H. R. Anderson, Jr., and R. B. Booth, "Materials/Processing Approaches to Phase Stabilization of Thermally Conductive Pastes," *IEEE Trans. Computers, Hybrids, & Manuf. Technol.* **13**, 713 (1990).
3. S. Iruvanti, R. K. Gupta, and E. Ruckenstein, "Stable High Solids, High Thermal Conductivity Pastes," U.S. Patent 5,098,609, March 24, 1992.
4. S. Iruvanti, K. S. Olsen, and K. G. Sachdev, "Polyester Dispersants for High Thermal Conductivity Paste," U.S. Patent 5,591,789, January 7, 1997.
5. T. Fiske, S. Railkar, and D. M. Kalyon, "Effects of Segregation on the Packing of Spherical and Non-Spherical Particles," *Powder Technol.* **81**, 57–64 (1994).
6. B. Bird, W. Stewart, and E. Lightfoot, *Transport Phenomena*, Second edition, John Wiley & Sons, New York, 2002, pp. 281–283.
7. J. W. Sinton, J. C. Crowley, G. A. Lo, D. M. Kalyon, and C. Jacob, "Nuclear Magnetic Resonance Imaging Studies of Mixing in Twin Screw Extruders," *Society of Plastics Engineers ANTEC Tech. Papers* **36**, 116–119 (1990).
8. R. Yazici and D. M. Kalyon, "Degree of Mixing Analyses of Concentrated Suspensions by Electron Probe and X-Ray Diffraction," *Rubber Chem. & Technol.* **66**, No. 4, 527–537 (1993).
9. R. Yazici and D. M. Kalyon, "Quantitative Characterization of Degree of Mixedness of LOVA Grains," *J. Energetic Mater.* **14**, No. 1, 57–73 (1996).
10. B. L. Greenberg, D. M. Kalyon, M. Erol, M. Mezger, K. Lee, and S. Lusk, "Analysis of Slurry-Coating Effectiveness of CL-20 Using a Novel Grazing Incidence X-ray Diffraction Method," *J. Energetic Mater.* **21**, No. 1, 185 (2003).
11. D. Kalyon, E. Birinci, R. Yazici, B. Karuv, and S. Walsh, "Electrical Properties of Composites as Affected by the Degree of Mixedness of the Conductive Filler in the Polymer Matrix," *Polym. Eng. Sci.* **42**, No. 7, 1609–1617 (2002).
12. D. M. Kalyon, A. Lawal, R. Yazici, P. Yaras, and S. Railkar, "Mathematical Modeling and Experimental Studies of Twin Screw Extrusion of Filled Polymers," *Polym. Eng. Sci.* **39**, No. 6, 1139–1151 (1999).
13. E. Birinci, R. Yazici, and D. M. Kalyon, "Statistics of Mixing Distributions in Filled Elastomers Processed by Twin Screw Extrusion," *Society of Plastics Engineers ANTEC Tech. Papers* **45**, 1720–1725 (1999).
14. D. Kalyon, H. Gevgilili, R. Yazici, A. Post, and G. McFann, "Flow and Structure Development Behavior of Bar Soaps Containing Synthetic Detergent," *Rheol. Acta* **43**, 396–405 (2004).
15. M. Zhang, "Introduction to Phase Change Thermal Interface Materials"; see *http://www.coolingzone.com/Guest/News/NL_JUN_2003/Dow/Dow_Jun_2003.html*.
16. R. S. Prasher and J. C. Matayabas, Jr., "Thermal Contact Resistance of Cured Gel Polymeric Thermal Interface Material," *IEEE Trans. Comp. Pkg. Technol.* **27**, No. 4, 702–709 (2004).
17. R. S. Prasher, "Rheology Based Modeling and Design of Particle Laden Polymeric Thermal Interface Materials," *Thermomechanical Phenomena in Electronic Systems—Proceedings of the Intersociety Conference (ITherm 2004)*, 2004, pp. 36–44.
18. R. S. Prasher, J. Shipley, S. Prstic, P. Koning, and J.-L. Wang, "Thermal Resistance of Particle Laden Polymeric Thermal Interface Materials," *J. Heat Transfer* **125**, 6 (2003).
19. R. S. Prasher, J. Shipley, S. Prstic, P. Koning, and J.-L. Wang, "Rheological Study of Micro Particle Laden Polymeric Thermal Interface Materials: Experimental (Part 1)," *ASME, Heat Transfer Div. HTD* **372**, No. 7, 47–51 (2002).
20. R. S. Prasher, J. Shipley, S. Prstic, P. Koning, and J.-L. Wang, "Rheological Study of Micro Particle Laden Polymeric Thermal Interface Materials: Modeling (Part 2)," *ASME, Heat Transfer Div. HTD* **372**, No. 7, 53–59 (2002).
21. I. Fisher, A. Siegmann, and M. Narkis, "The Effect of Interface Characteristics on the Morphology, Rheology and Thermal Behavior of Three-Component Polymer Alloys," *Polym. Comp.* **23**, No. 1, 34–48 (2002).
22. D. M. Kalyon, "Mixing in Continuous Processors," *Encyclopedia of Fluid Mechanics* **7**, Gulf Publishing, Houston, TX, 1988, Ch. 28, pp. 887–926.
23. D. Kalyon, "Review of Factors Affecting the Continuous Processing and Manufacturability of Highly Filled Suspensions," *J. Mater. Process & Manuf. Sci.* **2**, 159–187 (1993).
24. The functioning of three-roll mills is described, for instance, at *http://www.mixers.com/Proddetails.asp?ProdID=115*.
25. J. M. McKelvey, *Polymer Processing*, John Wiley & Sons, New York, 1962.
26. Z. Tadmor and C. G. Gogos, *Principles of Polymer Processing*, John Wiley & Sons, New York, 1979.
27. D. M. Kalyon, P. Yaras, B. Aral, and U. Yilmazer, "Rheological Behavior of a Concentrated Suspension: A Solid Rocket Fuel Simulant," *J. Rheol.* **37**, 35–53 (1993).
28. B. Aral and D. M. Kalyon, "Effects of Temperature and Surface Roughness on Time-Dependent Development of Wall Slip in Torsional Flow of Concentrated Suspensions," *J. Rheol.* **38**, No. 4, 957–972 (1994).
29. U. Yilmazer and D. M. Kalyon, "Slip Effects in Capillary and Parallel Disk Torsional Flows of Highly Filled Suspensions," *J. Rheol.* **33**, 1197–1212 (1989).
30. B. Aral and D. M. Kalyon, "Rheology and Extrudability of Very Concentrated Suspensions: Effects of Vacuum Imposition," *Plast. & Rubber Comp. Proc. & Appl.* **24**, 201–210 (1995).
31. D. Kalyon, H. Gokturk, P. Yaras, and B. Aral, "Motion Analysis of Development of Wall Slip During Die Flow of Concentrated Suspensions," *Society of Plastics Engineers ANTEC Tech. Papers* **41**, 1130–1134 (1995).

32. E. Bonaccurso, H.-J. Butt, and V. S. J. Craig, "Surface Roughness and Hydrodynamic Boundary Slip of a Newtonian Fluid in a Completely Wetting System," *Phys. Rev. Lett.* **90**, 144501-1–144501-4 (2003).
33. G. M. Carlomagno, "Heat Transfer Measurements by Means of Infrared Thermography," *Measurement Techniques*, von Karman Institute Lecture Series **1993-05**, Rhode-Saint-Genése, Belgium, 1993, pp. 1–114.
34. G. M. Carlomagno and L. de Luca, "Infrared Thermography for Flow Visualization and Heat Transfer Measurements," presented at the International Conference on Engineering Education, 1998; see *http://www.ctc.puc-rio.br/icee-98/Icee/Index.htm*.
35. R. D. Hudson, Jr., *Infrared System Engineering*, John Wiley & Sons, New York, 1969.
36. R. Siegal and J. R. Howell, *Thermal Radiation Heat Transfer*, second edition, Hemisphere Publishing Co., Washington, DC, 1981.
37. R. P. Madding, "Temperature Dependence of the Graybody Approximation to Emissivity for Some Common Materials," *Proc. SPIE* **4710**, 37–43 (2002).

Received September 22, 2004; accepted for publication April 13, 2005; Internet publication August 30, 2005

Claudius Feger *IBM Research Division, Thomas J. Watson Research Center, P.O. Box 218, Yorktown Heights, New York 10598 (feger@us.ibm.com)*. Dr. Feger is a Research Staff Member and manager of the Advanced Plastic Packaging group in the Electrical and Optical Packaging Department at the Thomas J. Watson Research Center. In 1976 he received a diploma in chemistry from Albert-Ludwigs University, Freiburg, Germany, and in 1980 a Dr. rer. nat. degree in polymer chemistry from the Macromolecular Chemistry Institute, Freiburg, Germany. After a visiting professorship in Porto Alegre, Brazil, and a postdoctoral assignment at the University of Massachusetts at Amherst, in 1984 he joined IBM at the Thomas J. Watson Research Center, where he has worked on various aspects of electronic packaging. In 1994 and 1999 he received IBM Research Division Awards, and in 1998 an IBM Microelectronics Division Award. He is an author or coauthor of 17 U.S. patents and more than 80 technical papers, and he has edited four books on polyimides. Dr. Feger is a past president (2002–2003) of the Society of Plastics Engineers (SPE) and has been a Distinguished Fellow of SPE since 1997. He is a member of SPE, the German Chemical Society, and IMAPS.

Jeffrey D. Gelorme *IBM Research Division, Thomas J. Watson Research Center, P.O. Box 218, Yorktown Heights, New York 10598 (gelorme@us.ibm.com)*. Mr. Gelorme is a Research Staff Member in the Advanced Plastic Packaging group in the Electrical and Optical Packaging Department at the Thomas J. Watson Research Center. He received a master's degree in polymer chemistry from the University of Massachusetts at Amherst. In 1982 Mr. Gelorme joined IBM, where he has worked on various aspects of lithography and electronic packaging. He is an author or coauthor of more than 20 patents and several papers, and is a member of the American Chemical Society.

Maurice McGlashan-Powell *IBM Research Division, Thomas J. Watson Research Center, P.O. Box 218, Yorktown Heights, New York 10598 (mmp@us.ibm.com)*. Mr. McGlashan-Powell is a Staff Engineer at the IBM Thomas J. Watson Research Center. He received a B.S. degree in physics from Wagner College in 1978 and then joined AT&T Bell Laboratories as a Member of Technical Staff working in the areas of optical materials research and radiation physics research. In his thirteen years at IBM, he has conducted research in the areas of infrared imaging and thermometry of microprocessors, magneto-optics, optical interconnect technology, thin-film metallurgy and interconnects, microprocessor circuit design, nanoscopic science, and low-temperature physics. Mr. McGlashan-Powell is the author or coauthor of ten publications and five U.S. patents.

Dilhan M. Kalyon *Stevens Institute of Technology, Castle Point Station, Hoboken, New Jersey 07030 (dkalyon@stevens.edu)*. Dr. Kalyon holds the Institute Professor Chair at Stevens Institute of Technology; he is the Founding Director of the Highly Filled Materials Institute. He has been with Stevens since 1980, upon obtaining his Ph.D. degree from McGill University, Montreal, Canada. Dr. Kalyon has more than 200 technical publications and five U.S. patents.